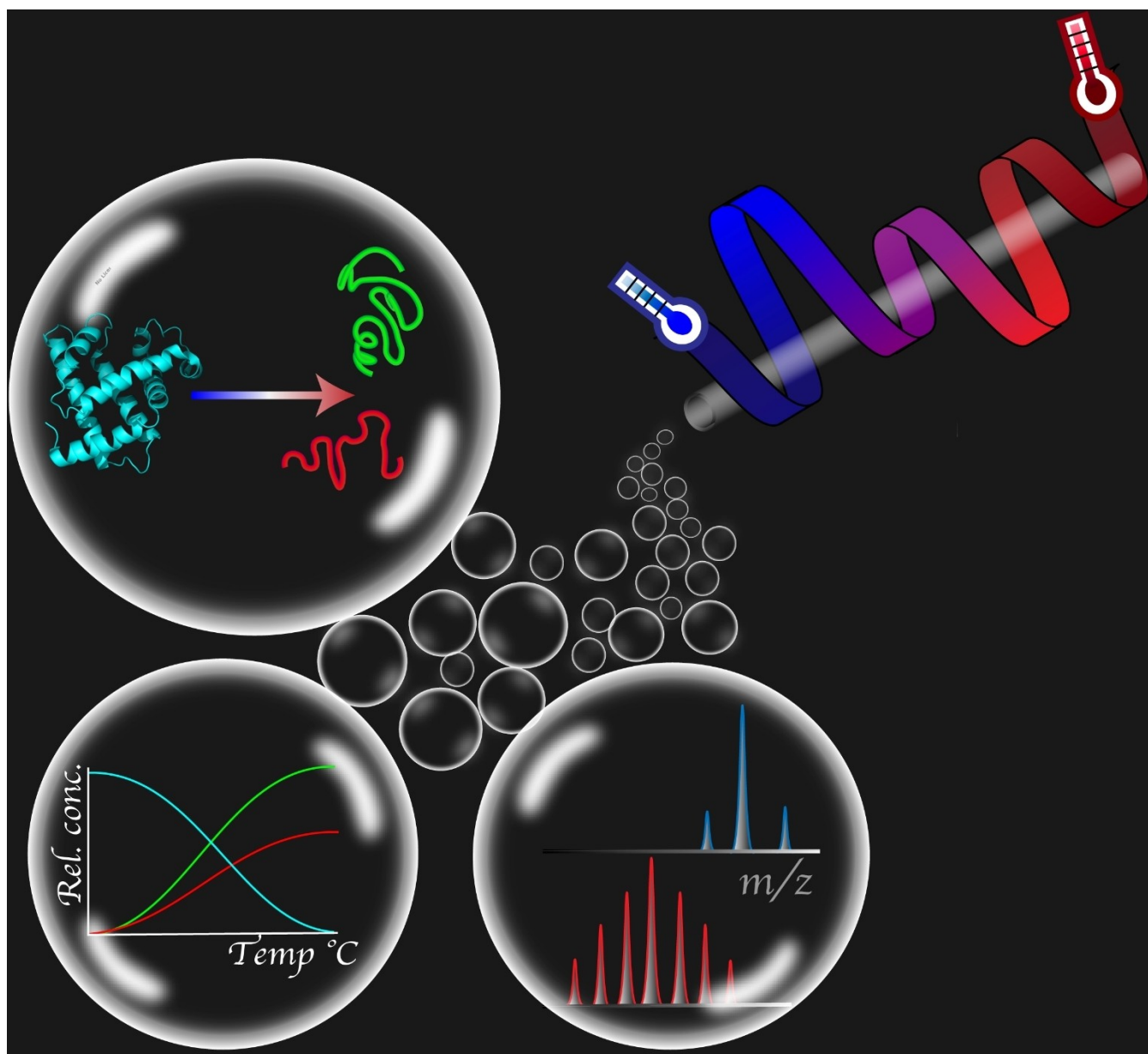


Special
Collection

Temperature-Controlled Electrospray Ionization: Recent Progress and Applications

Julian Alexander Harrison,^[a] Adam Pruška,^[a] Irina Oganessian,^[a] Philipp Bittner,^[a] and Renato Zenobi*^[a]

In memory of Prof. François Diederich, a great chemist with broad interest and knowledge and a wonderful friend and mentor.



Abstract: Native electrospray ionization (ESI) and nanoelectrospray ionization (nESI) allow researchers to analyze intact biomolecules and their complexes by mass spectrometry (MS). The data acquired using these soft ionization techniques provide a snapshot of a given biomolecules structure in solution. Over the last thirty years, several nESI and ESI sources capable of controlling spray solution temperature

have been developed. These sources can be used to elucidate the thermodynamics of a given analyte, as well as provide structural information that cannot be readily obtained by other, more commonly used techniques. This review highlights how the field of temperature-controlled mass spectrometry has developed.

1. Introduction

Investigating the energy landscapes of biomolecules presents several challenges. For example, the folding landscape of biomolecules is dictated by multiple noncovalent interactions, which, in turn, can lead to the formation of several intermediate states that are difficult to distinguish from each other. The ability to obtain information about these conformational states allows for the determination of their stabilities, as well as the kinetics of reactions. These data can be obtained by a range of the methods, such as circular dichroism (CD),^[1,2] isothermal titration calorimetry (ITC),^[3,4] and nuclear magnetic resonance (NMR).^[5] Another method that can be used for such an analysis is mass spectrometry (MS), which is the topic of this review.

Over the last 30 years, MS has become a powerful technique for analyzing biomolecules. The development of electrospray ionization (ESI) allowed researchers to transmit biomolecules from solution into a mass spectrometer, without major disruption to their structural architecture. Therefore, the data generated from this analysis gives a snapshot of what is occurring in solution. Native ESI can create ions of large, multi-subunit complexes, and in the context of biomolecular assemblies this field is sometimes referred to as 'gas phase structural biology'. A parallel technical development is temperature-controlled electrospray ionization mass spectrometry (TC-ESI-MS), which allows for the control of the spray solution temperature and has been used to investigate a range of molecular systems. Several source designs exist that can operate over a wide range of spray solution temperatures. Examples of these include several temperature-controlled (n) ESI,^[6–9] cold-spray ionization,^[10] high-pressure ESI,^[11] and dual heated-blocks source.^[12]

This minireview provides an overview of the biophysical methods that can be used to investigate the thermodynamic properties of biomolecules, and compares it with temperature-controlled ESI-MS. We also present the history, design, and development of TC-ESI-MS sources. How TC-ESI-MS has been used to analyze oligonucleotides, peptides and proteins is also discussed.

2. Biophysical Methods

Temperature-controlled MS complements many methods that can be used to investigate the thermodynamics, kinetics and/or structural properties of biomolecules (Table 1). These methods can be broadly grouped based on their underlying principles, with each possessing different strengths and limitations, which are discussed below.


2.1. Optical methods


Optical methods are based on interaction of photons with an analyte. This is measured in terms of scattering, absorbance, or fluorescence, where shifts in these observables are indicative of chemical or structural changes. Examples of these techniques include light scattering, circular dichroism (CD), UV/Vis, and fluorescence-based spectroscopies. Most spectroscopic instruments allow for the direct control of temperature while performing measurements. Therefore, they can be used to monitor temperature induced changes in biomolecules to elucidate their thermodynamic properties.

2.1.1. Light scattering

In dynamic light scattering (DLS) experiments, the scattering and intensity of photons is used to determine the hydrodynamic size of analytes within a given solvent. By subjecting the analyte to increasing temperatures, the change in their hydrodynamic size can be monitored, providing insights into their unfolding, melting, kinetics, or aggregation state.^[13] DLS instruments have built-in temperature control systems, allowing them to be used in high-performance unfolding experiments. However, these instruments have relatively low resolution and sensitivity for larger particles. Also, complex mixtures produce multiple light scattering events that are difficult to disentangle.

[a] Dr. J. Alexander Harrison, A. Pruška, I. Oganessian, P. Bittner, Prof. Dr. R. Zenobi
Department of Chemistry and Applied Biosciences
ETH Zurich
Vladimir-Prelog-Weg 3, 8093 Zurich (Switzerland)
E-mail: zenobi@org.chem.ethz.ch

 This article belongs to a Joint Special Collection dedicated to François Diederich.

 © 2021 The Authors. Chemistry - A European Journal published by Wiley-VCH GmbH. This is an open access article under the terms of the Creative Commons Attribution Non-Commercial License, which permits use, distribution and reproduction in any medium, provided the original work is properly cited and is not used for commercial purposes.

The scattering behaviour of impurities can also distort measurements.

2.1.2. Absorption spectroscopy

Circular dichroism is the most common spectroscopic method used to investigate the structural behaviour, thermodynamics, and stability of biomolecular complexes.^[1,14,15] This technique measures the absorbance of right- and left-circularly polarized light over a range of wavelengths. The molar absorptivity in a defined wavelength range (the molar circular dichroism), is reflective of the abundance of secondary or tertiary structure in solution. By screening for the change in absorbance with increasing temperature, CD can be used to detect changes in

the overall structure or a sub-structure of a molecule.^[1] An example of what this data looks like is shown in Figure 1, where the thermal denaturation of apolipoprotein was monitored CD. A drawback of this technique is that several physiological buffers cannot be used for CD experiments, as they absorb polarized light at the same wave lengths as secondary structures.^[39] A spectroscopic method which does not have this drawback is UV/Vis. This technique can be used to monitor structural changes in a biomolecule by measuring its absorbance at fixed wavelength(s). Changes in these absorbance measurements can be correlated with structural changes of the average sample mixture but cannot be assigned to secondary, tertiary, or quaternary elements. The sensitivity of UV/Vis melting experiments is further limited by the extinction of each

Irina Oganasyan has received her M.Sc. degree from York University (Toronto, Canada) in 2018 under the supervision of Prof. Derek Wilson. Currently, she is a Ph.D. student in a group of R. Zenobi at ETH Zürich, where she works on native mass spectrometry of non-covalent high-mass protein complexes.



Adam Pruška studied Analytical Chemistry in the group of Prof. Jan Preisler at Masaryk University, Brno, Czech Republic, where he received his M.Sc. in 2017. He pursued his master's project at Justus-Liebig University, Gießen, Germany working under the supervision of Prof. Bernhard Spengler. He worked on off-line coupling of separation methods with mass spectrometry, development of sample preparation for matrix-assisted laser desorption/ionization (MALDI) mass spectrometry and multimodal bioimaging of drug distribution in tumor spheroids. He later joined the group of R. Zenobi at ETH Zurich for his Ph.D. in mass spectrometry studying thermodynamics of nucleic acids and their non-covalent complexes.



Julian Alexander Harrison received his Ph.D. in Chemistry from the University of Wollongong in 2020, working under the supervision of Prof. Jennifer L. Beck and Dr. Celine Kelso. He was employed as a postdoctoral researcher at ETH Zürich in 2021 under the direction of R. Zenobi. Currently, he works on the characterisation of protein complexes by native and ion mobility mass spectrometry.



Philipp Bittner graduated from the University of Regensburg, Germany with a B.Sc. in Biology (2015) and M.Sc. in Biochemistry (2018). After finishing his first research project about photoresponsive enzyme complexes in the group of Prof. Reinhard Sterner, he joined the native MS team of R. Zenobi for his Ph.D. thesis (2020). His research focuses now on mass spectrometric investigations of modified collagen peptides, DNA-encoded chemical libraries, and of glycosylation patterns of antibodies.



Renato Zenobi has been full Professor of Analytical Chemistry at the Swiss Federal Institute of Technology (ETH) Zurich since the year 2000. After a Ph.D. at Stanford University and postdoctoral appointments at the University of Pittsburgh and at the University of Michigan, he returned to Switzerland in 1992 as a Werner Fellow at EPF Lausanne, where he established his own research group. Zenobi has made important contributions to the understanding of the ion formation mechanism in electrospray ionization (ESI) and matrix-assisted laser desorption/ionization (MALDI) mass spectrometry, to the development of analytical tools for the nanoscale, in particular, tip-enhanced Raman spectroscopy (TERS), and to exhaled breath analysis by using ambient ionization methods.



Table 1. Well-established biophysical methods used to investigate structural, binding, thermodynamic, and kinetic properties of biomolecules and their complexes.

Method	Output Information	Main Advantages	Main Disadvantages	Sample Amount	References
Circular dichroism (CD)	Tertiary/secondary structural composition, conc., T_m , ΔH° , ΔC_p	Label-free, access to structural information, thermodynamics	CD buffer required, low throughput, high sample amount, time consuming	several μg per measurement (μM range)	[1,14,15]
Ultraviolet/visible spectroscopy (UV/Vis)	Structural stability, conc., purity, T_m , k_{cat}^* [a], K_M^*1 , K_d and derived ΔH , ΔG , ΔS	Label-free, high flexibility in selection of buffer system	UV/Vis absorption of sample required, overlap if signals	several μg per measurement (μM range)	[16–18]
Nano differential scanning fluorimetry (nDSF)	$T_m^*1,2$	High throughput (capillary based), label-free, low sample amount	Tryptophan or tyrosine residues required	nM to μM (few μL)	[19–21]
Microscale thermophoresis (MST)	multiple K_d and derived ΔH , ΔG , ΔS stoichiometry, oligomerization and aggregation	High throughput (capillary based), low sample amount	Fluorophore labelling required	nM (several μL)	[19,22,23]
Fluorescence polarization (FP)	K_d and derived ΔH , ΔG , ΔS	High throughput (in well plates), low detection limit	Quenching and light scattering interferences, autofluorescence	nM to μM (several μL)	[24–26]
Dynamic light scattering (DLS)	Size, viscosity, T_m	Low sample amount, particles from 0.1 nm to 1 μM can be measured	Low resolution, particle impurities may affect measurement	several μg (μM range)	[13,27,28]
Surface plasmon resonance (SPR)	k_{on} , k_{off} and derived K_d	Low sample amount, label-free, access to k_{on} and k_{off}	Immobilization required - interferes with binding event, no direct structural information	several μg (μM range)	[29–31]
Nuclear magnetic resonance spectroscopy (NMR)	Detailed structural information, unfolding/folding kinetics, T_m , ΔH and ΔC_p	Atomic structural resolution, multi-dimensional experiments, non-destructive	High sample amount, time consumption of ^{13}C NMR	several mg	[5,32,33]
Differential scanning calorimetry (DSC)	T_m , ΔH and ΔC_p	Low sample amount, liquid and solid phase analysis, sample (im)purities	Reference material required (sample cell), high sample amount	several μg per measurement (μM range)	[34–36]
Isothermal titration calorimetry (ITC)	K_d , ΔC_p and derived ΔH , ΔG , ΔS	Label-free, access to TD information	Buffer limitations, high sample consumption, low sensitivity	μg -mg per binding assay (μM range)	[3,4,37]
Native mass spectrometry (MS)	Charge states, oligomerization, conc., unfolding/folding kinetics, stoichiometry, T_m , K_d and derived ΔH , ΔG , ΔS	Very high sensitivity, label-free, parallel monitoring of complex mixtures	Gas phase environment, strict buffer/salt limitations may affect native state of sample	pg (low μM range)	[7,9,38]

Applicable only for proteins [1], peptides [2], oligonucleotides [3].

sample. Therefore, peptides or proteins not possessing tryptophane or tyrosine residues cannot be measured.^[16–18]

2.1.3. Fluorescence spectroscopy

The drawback of both CD and UV/Vis is that they are low throughput methods that require a large amount of sample. To overcome the need for large amounts of sample, novel capillary-based methods such as nano differential scanning fluorimetry (nDSF) were developed. This technique is used to monitor changes in tryptophan or tyrosine fluorescence. The amount of fluorescence depends on the number of exposed amino acids in solution such that protein unfolding can be inferred from an increase in fluorescence. Melting curves can be generated using this nDSF by measuring the fluorescence ratio of wavelengths 330 to 350 nm with increasing temperature. The resulting melting curves allow the determination of T_m or

thermodynamics of a protein. As tryptophan or several tyrosine residues are required for nDSF, this technique is limited to certain proteins and several peptide complexes.^[19,23]

Another capillary-based method that can be used to investigate the thermodynamics of biomolecules is microscale thermophoresis (MST). This technique uses an IR laser to heat a sample that has been placed within a capillary. The analyte's movement along the laser-induced temperature gradient are monitored. Changes in the size, charge or conformation are determined by measuring either the intrinsic (tryptophan residues) or extrinsic (fluorophore labelled) emitted fluorescence of the analyte.^[19] These experiments can be performed sequentially in multiple capillaries, allowing for the rapid screening of different solutions. The prerequisite for making label-free measurements is that a substantial change in intrinsic fluorescence is required. If this cannot be achieved, a covalently bound fluorophore needs to be attached.^[19] This

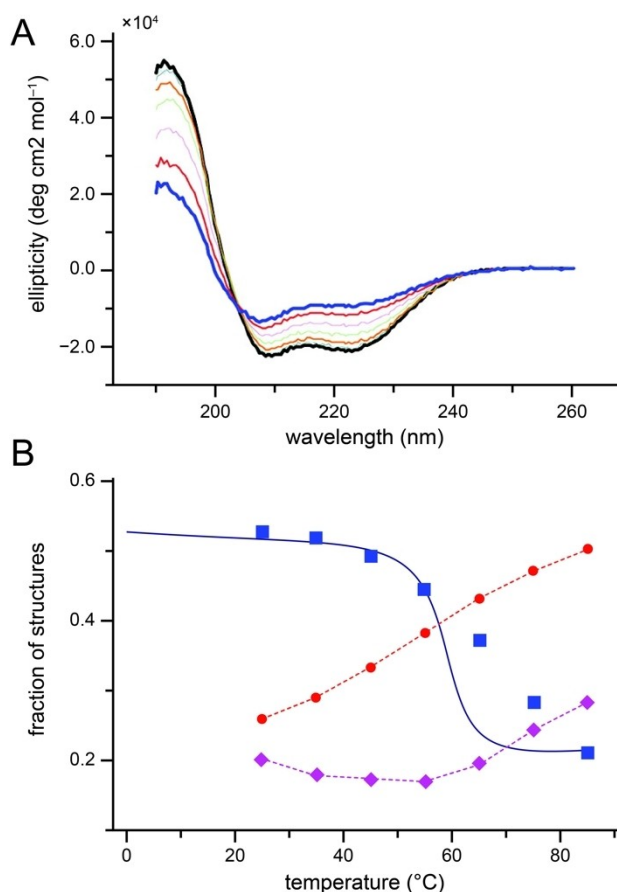


Figure 1. (A) CD thermal unfolding of recombinant Apolipoprotein A-I (Apo A-I, 0.5 mg mL⁻¹ in 100 mM NaF and 10 mM Na₃PO₄ at pH 7.4) CD spectra of Apo A-I for temperatures between 25 °C (black line) and 85 °C (blue line) recorded in 10 °C steps. (B) Deconvoluted CD spectra of wavelengths representing three structural elements: (■) α -helix, (●) β -sheet, and (◆) random coil. Curves demonstrate that the loss of α -helical occurs with an increase in β -structure content. The solid blue line is calculated α -helix content using Zimm-Bragg theory. Reprinted with permission from *Biochem. J.* 51 (2012) 1269.^[40] Copyright © 2021, Wiley-VCH.

technique has been used to determine the dissociation constants (K_d) of (membrane) protein-ligand systems with K_d values down to the pM range.^[22,23]

Fluorescence polarization (FP) represents a sensitive and high-throughput fluorescence-based technique that can be used to investigate the binding affinities and the thermo stability of proteins or protein-ligand complexes. For this method, the sample that is either intrinsically fluorescent or needs to be labelled with a fluorophore, is excited with polarized light. Depending on the rotational motion on the timescale of fluorescence emission, the fluorophore emits polarized or depolarized light. The ratio of emitted polarized and depolarized fluorescence light can be correlated to a binding event or to the degree of biomolecular folding. However, there are a few things that need to be considered when using these techniques to investigate the thermodynamics of biomolecules. First, conjugating fluorophores to an analyte may interfere with biomolecular folding. Also, these experiments can only be performed over a limited range of

temperatures, since the fluorophores used in these assays are temperature sensitive.^[24,25] Finally, quenching, light scattering and/or autofluorescence can disrupt measurements.^[26]

2.1.4. Resonance spectroscopy

Surface plasmon resonance (SPR) is an affinity-based method that became one of the gold standards for evaluating protein-protein, protein-ligands and DNA interactions. This technique works by reflecting light near the critical angle from a plasmonically active (gold) surface, which carries the immobilized sample of interest on the solution side of the interface. Intensity and angular changes of the reflected light (caused by plasmon resonances) can be directly correlated to binding or dissociation events and give access to the analyte's k_{on} and k_{off} . However, this technique has two major drawbacks. How the ligand is attached to the gold surface may change its structure as well as affect the binding of the analyte.^[29] Also, the detection of plasmonic resonance is highly temperature sensitive, so only one temperature point can be measured per an experiment.^[29–31]

Nuclear magnetic resonance (NMR) spectroscopy is a prominent, high resolution method which is mainly used to investigate the structure of biomolecules.^[32] Combining 1D and 2D ¹H and ¹³C NMR experiments, this non-destructive technique allows noncovalent interactions to be elucidated and its binding kinetics to be determined.^[5] Temperature jump NMR can be used to monitor the temperature induced unfolding of a biomolecule, as well as generate high resolution structures of folding intermediates.^[33] However, it should be noted that NMR analysis is limited by the need for isotope labelling (e.g., ¹³C, ¹⁵N) for certain NMR experiments, sample availability, low throughput and laborious data analysis, which increases exponentially with the size of the biomolecule under study.

2.2. Calorimetric methods

Calorimetric approaches have been widely used by biophysicists and organic chemists to determine the binding affinities, enthalpy changes, stoichiometry and molecular interactions for a wide range of molecules.^[34] An example of a calorimetric method which is used to investigate biomolecules is differential scanning calorimetry (DSC). This technique can be used to monitor endothermic enthalpy changes over a range of temperatures by detecting the unfolding of biomolecules. However, this technique does not provide any other structural data.^[35] In contrast, isothermal titration calorimetry (ITC) can be used to determine affinity constants, reaction or unfolding enthalpies, as well as stoichiometries of a biomolecule at a fixed temperature.^[37] The core strength of ITC is that it is a label-free method, however, it consumes large amounts of sample, as an excess of the titrant is necessary for each experiment.^[3,4]

2.3. How these techniques compare to TC-ESI-MS

The development of temperature-controlled sources has allowed MS to be used to investigate the thermodynamics of biomolecules. Compared to most of the solution-based techniques described above, TC-ESI-MS has lower sample consumption, and except for NMR, can provide more detailed structural information. Also, complex mixtures or impurities further impede the output information of most optical and calorimetric methods, as the detection signal only represents an average of the sample solution. Most of these obstacles are overcome with TC-ESI-MS, which is able to monitor T_m , thermodynamics, or structural changes in a complex mixture of analytes in parallel.

However, measurements made in the gas phase do not always perfectly reflect the solution composition and equilibria, therefore it is advantageous to use TC-ESI-MS in conjunction with a solution-based technique, such as absorption spectroscopy (e.g., UV/Vis), fluorescence methods (e.g., FP) or target immobilization (e.g., SPR). These attributes make TC-ESI-MS a powerful, complementary technique, whose output cannot be observed by most other methods. For example, the easy accessibility of CD spectroscopy to T_m , tertiary and secondary structural information complements TC-ESI-MS data. An example is given in Figure 2, which shows the heat transition of human antithrombin (AT), a 57 kDa monomeric protein analyzed by DSC and TC-ESI-MS.^[36] Both techniques were used to determine the T_m of human antithrombin. While both T_m calculated using these techniques were in good agreement with each other (Figure 2A), DSC was not able to reveal any insights of AT conformational changes occurring above the transition temperature of $56 \pm 1^\circ\text{C}$. A second DSC scan could only prove the heat-locked transitional state. However, TC-ESI-MS showed that human antithrombin forms dimers and trimers at temperatures above 55°C with the appearance of novel charge state distributions. The ion peaks corresponding to these multimers can be observed in the 60°C and 65°C spectra, in the m/z region 5000 to 7000 (Figure 2B).^[36] These results demonstrate the power of TC-ESI-MS, highlighting its ability to detect temperature induced oligomerization occurring in solution.

Temperature-controlled sources are designed to heat or cool the analyte in solution prior to being sprayed. This provides a “snap-shot” of the conformations the analyte adopts in solution for a given temperature. By performing the measurements over a range of temperatures, the thermodynamic characteristics of a biomolecule, such as the melting temperature, can be determined. The results obtained by all the TC-ESI-MS have been shown to be in good agreement with other solution-based techniques. However, despite the agreement with solution-based measurements, the effects of temperature on the electrospray process should be discussed.

Biomolecules in solution are desolvated after being sprayed by ESI following different pathways. For example, for folded proteins, the solvent is evaporated around them, and eventually only the exposed ionisable amino acids on the proteins surface retain a charge (charge residue model). Conversely, denatured proteins are ejected from the droplet as a chain, and the ionisable amino acids on the chain gain a charge (chain ejection

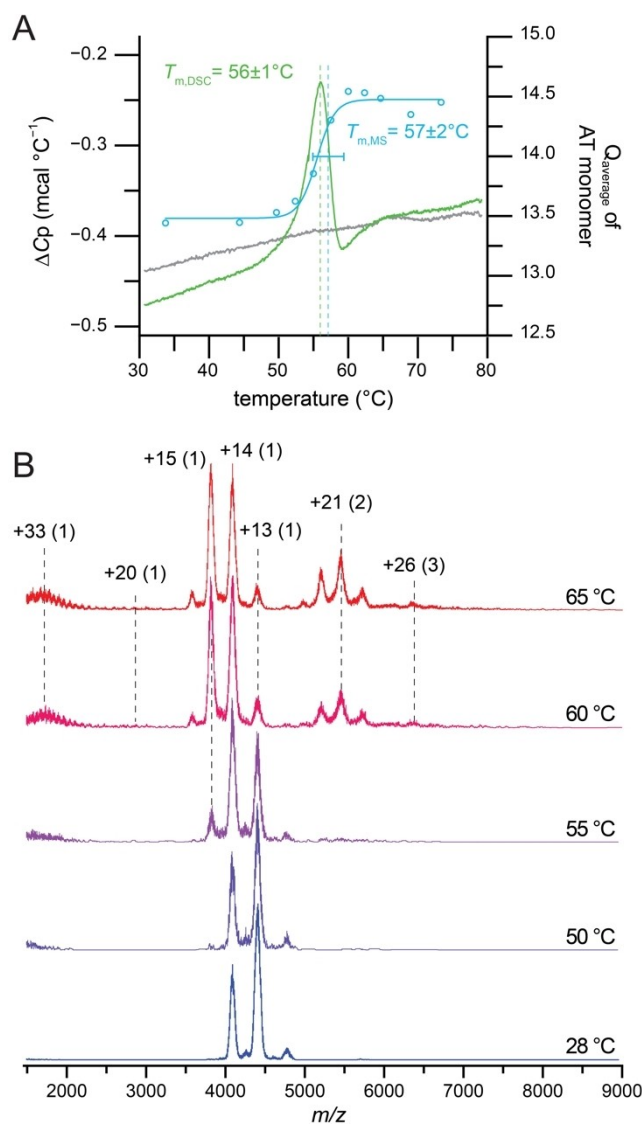


Figure 2. Thermal denaturation of human antithrombin (AT; 57 kDa; in 150 mM NH_4Ac , pH 8.0). (A) The average charge state of AT vs. temperature (blue) overlaid with the DSC thermogram (green) is plotted. The horizontal error bar represents the standard deviation of $T_{m,MS}$ derived from three experimental repetitions. The flat gray trace represents the thermogram of a second DSC scan indicating that AT undergoes irreversible conformational changes. (B) ESI mass spectra of AT colored according to different temperatures between 28 – 65°C . The peak labels indicate ionic charge states. The oligomeric states are shown in parentheses.^[7] Compliments of Guanbo Wang (Nanjing Normal University) and Igor A. Kaltashov (University of Massachusetts).

model).^[41] Partially folded proteins have been proposed to follow an intermediate desolvation mechanism (partial ejection model).^[42] Since the number of charges a protein carries is dependent on how folded/globular it is in solution, its average charge state, as measured by MS, can therefore be used to assess how folded it was in solution. The charge state distribution can thus be used as a proxy for native vs. denatured state of biomolecules.

However, during TC-ESI-MS experiments, increasing the temperature of the solution will affect its viscosity, and there-

fore the size of initial the droplets formed during electrospray as well as their charge.^[43–45] One could argue that biomolecules contained within smaller droplets would carry less charge and appear more native like in the mass spectra, opposite to the expected unfolding as temperature increases. However, given how well the TC-ESI-MS results match those obtained using solution-based methods, it is unlikely that these effects play a major role in the charge state distribution or conformations proteins adopt while using this technique.

3. Ion Source Designs

The earliest design of a temperature-controlled ion source for mass spectrometry was published by Natagawa and Katsugari in 1958,^[46] predating even the development of ESI by a decade.^[47] Although there were some developments in the 1980s for temperature-controlled ESI sources (thermospray),^[48] the first publications utilizing temperature control sources to analyze biomolecules were published in the early 1990s. Since then, multiple source designs have been developed by different labs, which have been used to investigate a range of oligonucleotides, peptides, and proteins. The development, design, and capabilities of these temperature-controlled sources is discussed in this section.

3.1. Sources for thermodynamics

3.1.1. Heating by an airflow

The earliest TC-ESI-MS source used to investigate biomolecules was published in 1991 by Le Blanc et al.^[49] This design utilized a modified 1500 W hot-air gun to heat the spray probe/interface region, and was first used to investigate the thermal denaturation of cytochrome c. Another iteration of this design was published in Cong et al., where it was used in ligand binding studies with membrane proteins.^[50] This system utilizes two fans, which directed air from a heatsink chamber towards the ion source. To produce the hot airflow, ambient air is brought into a heatsink chamber, which is mounted on a Peltier thermoelectric chip. The Peltier allows for the precise control of air temperature (T_{air}). Once heated, the air is directed towards the ion source region, where the T_{air} near the nESI capillary is monitored with a probe. To ensure the desired sample temperature (T_{sample}) was reached, the system needed to be calibrated. This was done prior to experiments using a second micro-thermocouple, which was inserted into the nESI emitter. This calibration curve was used to determine the relationship between T_{air} and T_{sample} . It should be noted that the micro-thermocouple was not used to monitor the temperature of solutions containing the analyte, to avoid contamination. For this source design, it takes approximately 40 seconds T_{sample} and T_{air} to reach equilibrium after placing the nESI emitter into the source chamber.^[51] Due to the equilibration times, this source cannot be used to perform continuous experiments, also,

thermal titration experiments contain a limited number of data points.

3.1.2. Wire heating

The earliest wire heating source design was first proposed in 1993 by Mirza et al., where it was used to investigate the thermal denaturation of cytochrome c.^[52] In this source design, an ESI emitter and a thermocouple were placed in separate holes within a ceramic rod, which had a chrome wire wrapped around it. An electrical current could be applied to the chrome wire using a low-voltage power supply to change the ceramic rods temperature. A thermocouple was used to monitor the ceramic rod, and by proximity, spray solution temperature. This heat wire source configuration allowed the spray solution temperature to be set between 25 to 96 °C.

The ceramic rod insulates the ESI capillary (~3 kV) from the heating wire (~5 V) so it does not interfere with the electrospray process. However, since the thermocouple is so close to the ESI emitter in this design, it can disrupt the electrospray when active. Therefore, the spray solution temperature cannot be monitored during electrospray experiments. Another drawback of this design is that the temperature needs to be equilibrated for at least 2 minutes prior to analysis, thus, continuous experiments cannot be performed. A later study modified the design reported in Mirza et al. to fit a nESI source coupled with a Fourier-transform ion cyclotron resonance mass spectrometer, where it was used to investigate temperature-induced conformational changes in proteins.^[53]

3.1.3. Heating with a metal block

The most common TC-ESI-MS source designs use heated metal blocks to control temperature, with several designs being used by researchers. The first publication reporting a metal heat block TC-ESI-MS source was published by the Robinson lab.^[9] This design uses a thermoelectric cooler (TEC), as well as a Peltier element to control the nESI capillary temperature. The TEC and the nESI capillary are fitted between two aluminum blocks, which allows for rapid heat transfer. Both the TEC and a heat sink are electrically insulated from the block with a thermally conductive, electrically nonconductive sheet held in place with nylon screws. This was done to prevent the electrospray voltage from producing sparks and short circuiting the source. This source design also allows spray solution temperature to be changed during the electrospray experiments, thus, allowing for continuous measurements to be made.

A similar metal block source design was developed and patented by the Kaltashov lab.^[7,55] This temperature-controlled source has been used to investigate multiple proteins and nucleic acids. The T_m obtained using this source are similar to those calculated by DSC (data shown in Figure 2). The Kaltashov design uses copper instead of aluminum, and the metal block is fitted around an elongated, S-shaped ESI emitter. These design choices were made to improve heat transmission and efficiency.

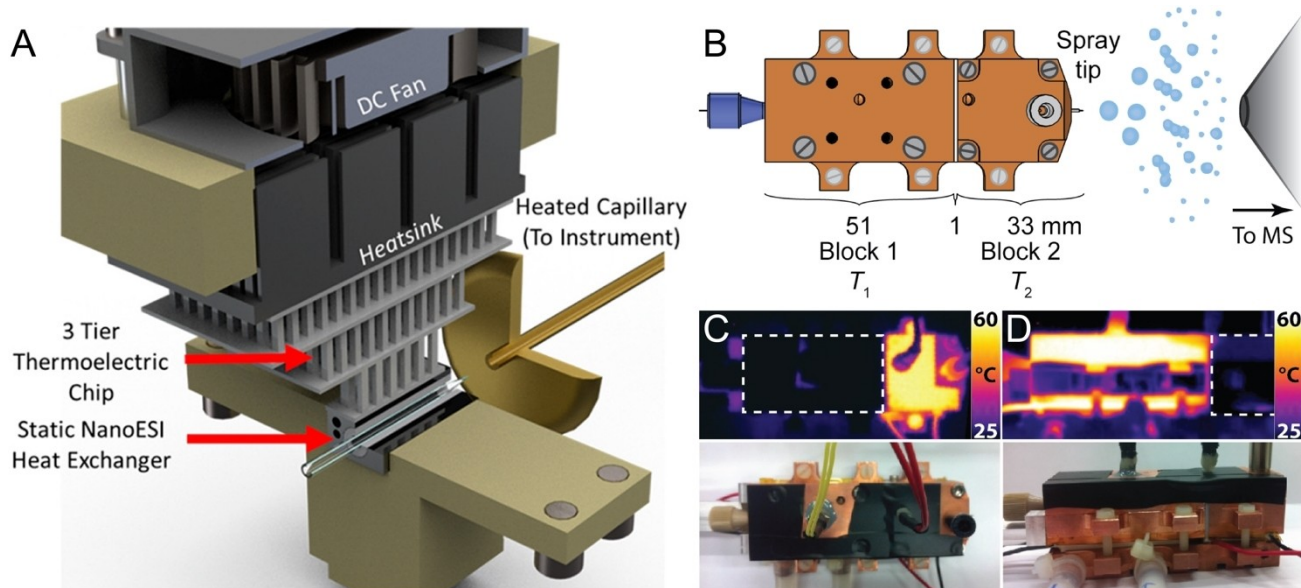


Figure 3. Recent experimental designs of (A) a three-tier temperature-controlled ESI source and (B–D) a temperature-jump ESI source. The design shown in (A) allows temperatures from ~ 5 – 98 °C to be reached, with an accuracy of ± 2 °C in most of the temperature range. The design shown in (B) subjects a flow of sample to a temperature jump, either from cold to hot (C), for example, for following “melting” of a complex, or from hot to cold (D). The flow rate dictates how much time the sample spends in the hot and cold regions of the device, and measurements with different flow rates allow one to get kinetic information. Part A reprinted with permission from *Anal. Chem.* 93 (2021) 6924.^[12,54] Copyright © 2021, Wiley-VCH.

Elongation of the ESI emitter allowed for a prolonged spray time compared to other TC-ESI-MS sources. Because ESI is used instead of nESI, the memory effect on protein folding, as well as the decrease in spray solution pH during long experiments is avoided.

After the Kaltashov design was published, several other nESI design that allowed temperature control were developed. These nESI sources were used to investigate conformational changes occurring during the thermal denaturation on cytochrome *c*,^[56] as well as elucidate multiple stable, intermediate structures of ubiquitin^[6] and bovine serum albumin.^[57] The intermediate states of DNA complexes have been investigated using a similar design coupled with IMS by Hommersom et al.^[58] This design has been shown to be a useful tool for probing the thermodynamics and ligand binding of non-canonical nucleic acid structures, as shown in Marchand et al. The source modifications made in this latter study allowed for the real-time control of temperature ramps, with one scan performed every second. This was achieved using a LabView code in conjunction with a PID controller.^[38] Recently, a TC-ESI-MS source which uses a three-tier Peltier TEC design was described in McCage et al.^[54] This source allows for the spray solutions to be set between 5 to 98 °C. A schematic of this design is shown in Figure 3A. This source uses the air around the TC-ESI to control the temperature of the ESI emitter, which is necessary for preventing condensation at low temperatures below 15 °C. This source is also designed to minimize the air turbulence, which disrupts the electrospray. The three-tier Peltier TEC provides a much-improved performance over single-tier Peltier TEC designs.

3.1.4. Laser heating

A recent study from the Clemmer lab presented a laser-based temperature-controlled source.^[59] This design uses a variable-power, 10.6 μm CO₂ laser to rapidly heat nanodroplets produced during ESI. This laser source shares some design elements with laser ablation electrospray ionization (LAESI).^[60] The main difference between these approaches is the laser wavelength and a sample location. The far infrared CO₂ laser rapidly heats droplets containing sample, generated by a regular ESI source. Sample heating using a laser occurs on a μs timescale, which is several orders of magnitude faster than TC-ESI-MS, allowing for an analytes structure to be investigated in a pre-equilibrium state. Laser heating has been used to identify structural intermediates of myoglobin, and has the potential to elucidate other aspects of protein folding.^[61]

3.2. Comparison of source designs

At the time of writing this review, there were no commercially available TC-ESI-MS sources. Many labs have been able to replicate and modify source designs based on schematics from published literature (references given in Table 2). Many of the sources have similar designs and are used for similar applications, thus they are briefly compared in this section. The sources described in section 3.2. were excluded from comparison, due to how dissimilar they are from the other designs. Most of the sources have similar temperature range (Table 2), and the modern designs have a temperature accuracy of ± 1 °C. A significant difference between designs is that the metal block,

Table 2. Timeline of the development of temperature-controlled sources.

Year	Principle	Source	Temp. Range [°C]	Ref.
1991	hot-air gun	ESI	25–92	[49]
1993	heating wire	ESI	25–96	[52]
1998	heating wire	nESI	25–90	[53]
2000	cold-spray ionization*	ESI	–80–15	[62]
2003	heated block (Al)	nESI	10–90	[9]
2011	heated block (Cu)	ESI	26–90	[7]
2014	heated block (Cu) + high pressure ^[a]	nESI	up to 180	[63]
2016	hot-air gun	nESI	25–40	[50]
2017	heated block (Al)	ESI	25–92	[6]
2018	heated block (Cu)	nESI	5–95	[38]
2020	two heated blocks (Cu)	ESI	5–95	[12]
2021	CO ₂ laser ^[a]	ESI	0–30 W ^[b]	[64]
2021	Multi Peltier elements	nESI	5–98	[54]

[a] Ion sources operating outside the standard temperature range (0–100 °C); [b] laser energy is used instead temperature.

CO₂ laser and multi-Peltier sources can perform continuous measurements, while the others can only be used for discontinuous measurements. As mentioned in section 3.1. the heating wire and hot-air gun designs also have significant drawbacks compared to the metal block designs, in terms of temperature maintenance and equilibration times while performing experiments. The source with the fastest sample heating is the laser source, as discussed above.

3.3. Special ion sources

Most TC-ESI-MS source designs can perform experiments at temperatures between 20 to 100 °C. Also, they can only apply a single temperature to the spray solution at a given time. However, there are a few source designs that can perform experiments outside of these typical conditions. This section focuses on temperature-controlled ionization sources that have been designed to investigate the analytes under atypical solution conditions.

3.3.1. Cold-spray ionization

A source configuration which can analyze supramolecular complexes at temperatures below the freezing point of water is cold-spray ionization (CSI).^[62] This source was designed by the Yamaguchi lab, and is capable of setting the spray solution temperature between –50 to 15 °C. These temperatures are achieved by using liquid nitrogen to cool the source, as well as cold N₂ as a sheath gas. To prevent the ESI probe from freezing at temperatures below 0 °C, acetonitrile is added to the spray solution. Several studies have been published which used CSI to analyze proteins^[65] and dsDNA.^[66,67]

3.3.2. High-pressure sources

There are also source designs that allow for solvent temperatures to exceed the boiling point of the solvent. Under atmospheric conditions, such temperatures would generate bubbles, which disrupt the electrospray process. This issue can be overcome by keeping the source pressure high enough that the spray solution cannot boil. This is the underlying principle of super-heated high-pressure ESI, which is described in Chen et al.^[68] In this design, the ion source chamber can maintain an internal pressure up to 11 atm, which allows the experiments to be performed at temperatures up to 180 °C.^[63] Besides hydrophobicity and viscosity, the surface tension, as well as the dielectric constants and the concentration of H₃O⁺ and OH[–] ions change dramatically when water is heated above 100 °C. When the temperature increases above 200 °C, water has solubility properties similar to those of hydrophobic organic solvents.^[69] Remarkably, this method can work with less-polar compound, such as membrane proteins, which becomes soluble in the subcritical water at high temperature. This system has also been coupled with high-temperature HPLC, presenting a new avenue of peptide separation and fragmentation to proteomics researchers wanting to investigate the less-polar fractions directly after HPLC separation, without boiling the mobile phase or creating an electrical discharge.^[70]

3.3.3. Temperature jump source

The temperature jump source has been developed recently, and was published in 2020 by Marchand et al.^[12] This design allows for the analysis of analytes after a fixed cooling or heating period. A schematic of this source is shown in Figure 3B. This source utilizes a dual block ESI temperature-controlled system. The temperature of each copper block is controlled independently, creating separate temperature regions within the ESI emitter. The first, longer block is used to equilibrate the sample at a temperature T₁. When the solution enters the second block set at a different temperature T₂, the equilibrium of the analyte changes. At the exit of the second block, the solution is electrosprayed as with a pneumatically assisted ESI source. The time that that sample spends at T₂ can be controlled by varying the solvent flow rate, allowing this source to be used to investigate the kinetics of biomolecular equilibria (k_{on} , k_{off}).

4. Applications to the Analysis of Biomolecules

TC-ESI-MS has been used to investigate a wide range of biomolecules. The data obtained from using this technique has provided great insights into the biophysical characteristics of the multiple proteins, peptides, and oligonucleotides. Most of the data collected using TC-ESI-MS have provided novel insights into the temperature-induced structural changes in biomolecules, which are discussed below.

4.1. Proteins

In the early 1990s, several mass spectrometry studies were performed using pH titration, which demonstrated that, for a given protein, a shift to higher charge states is indicative of unfolding.^[71–73] Utilizing this information, researchers developed the first ESI sources capable of controlling spray solution temperature. This led to the development of multiple TC-ESI-MS source designs, which are listed in Table 2.^[7,9,74–76] These sources have been used to investigate the biophysical properties of multiple proteins. One of the first studies applying TC-nESI to investigate the thermal behaviour of noncovalent complexes was done by the Robinson lab in 2003.^[9] In this work, the T_m of lysozyme (Figure 4A and B) and TaHSP16.9 (Figure 4C) were calculated. Also, the temperature dependent subunit equilibrium of TaHSP16.9 was investigated. These data provide an example of how mass spectrometry data can be used to derive the thermodynamic properties of a biomolecule.

The TC-ESI-MS data for lysozyme illustrates how this technique can be used to derive thermodynamics information.^[9] The spectrum acquired at a temperature of 25 °C shows three charge states in the m/z region 1400 to 1800 (Figure 4A). The spectra acquired at higher temperatures contain higher charge states for lysozyme, which can be observed in the m/z region 1150 to 1350. This is because, as temperature increases, lysozyme begins to unfold, exposing more amino acid residues that can be protonated to solution. This shows that the charge

state distribution of a biomolecule reflects the degree of folding/unfolding it is in solution. When average charge state (Q_{average}) of lysozyme was plotted against temperature, it gave a melting curve (Figure 4B). The T_m of lysozyme derived from this melting curve was 43.0 ± 0.6 °C, which is in a good agreement with fluorescence measurements made under the same solution conditions.^[9]

This analysis was also performed on TaHSP16.9, a dodecameric small heat shock protein assembly. The thermal denaturation of this protein complex produced a variety of dissociation products (predominately monomers and dimers, seen in the m/z region 1000 to 4000 of the mass spectrum, Figure 4C). However other oligomers, such as undecamers and tetradecamers, were also observed in the mass spectra. This study demonstrated that TC-ESI-MS can be used to determine the melting temperatures of proteins, as well as provide insight into thermally induced structural changes in multi-subunit complexes. The latter cannot be examined by most other biophysical techniques use to study thermodynamics This research, in conjunction with similar work, set the stage for applications to more complex systems.^[7,9,74–76] Examples of these include utilizing ion mobility spectrometry (IMS) to investigate the of transition states of proteins during melting experiments,^[6,56,57,61,77] investigations of the thermodynamics of ligands like lipids^[78] or metal co-factors binding to biomolecules^[61,79], temperature-induced conformational transitions of antibodies,^[36,80] structural transitions during oligomeric

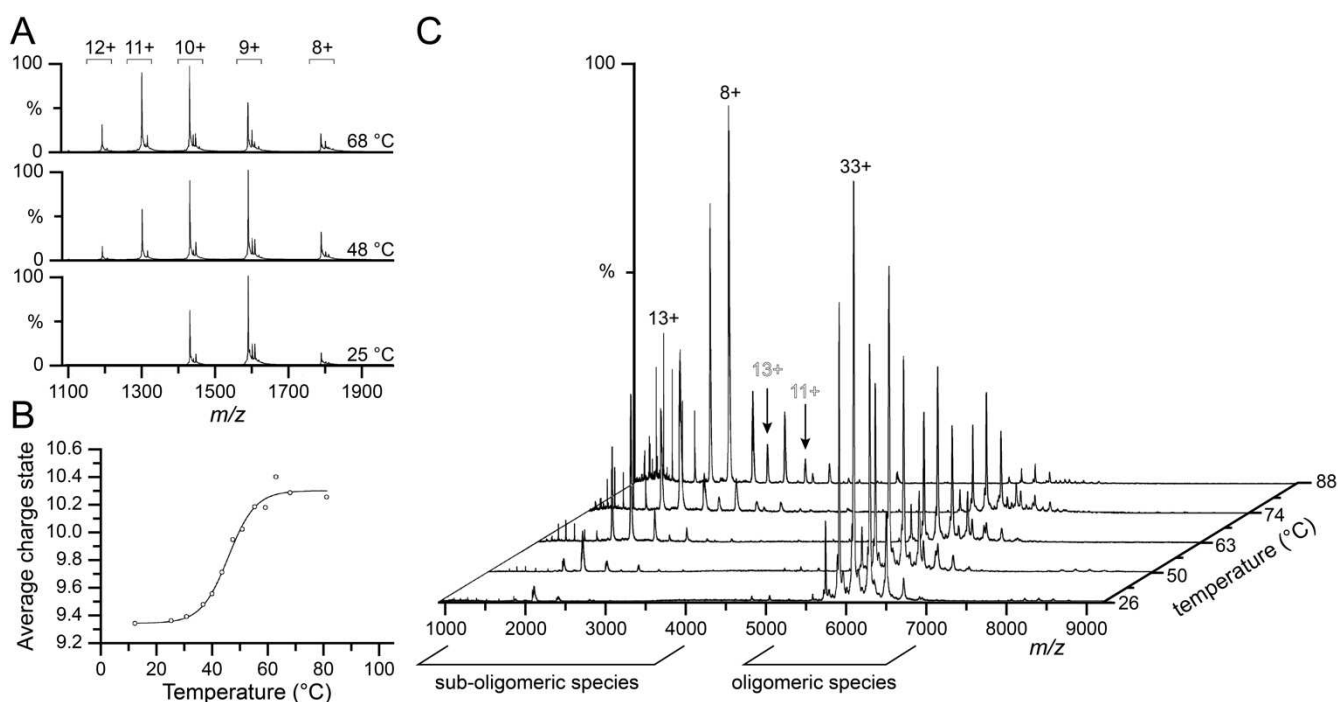


Figure 4. (A) Mass spectra of hen egg white lysozyme at 25 °C (bottom), 48 °C (middle), and 68 °C (top). A charge state distribution shift towards higher charges with increasing temperatures indicates unfolding of the protein structure. (B) Dependence of average charge state (Q_{average}) vs. temperature measured by an embedded thermocouple showing $T_m = 43.0 \pm 0.6$ °C (inflection point). (C) Mass spectra representing dissociation of a wheat heat shock protein, TaHSP16.9, using TC-nESI-MS. Spectra at different temperatures show the dissociation on the oligomeric species (dodecamer, ~6000 m/z) into suboligomeric species (at 1000 - 4000 m/z). Selected charge states for monomers (solid type) and dimers (outlined type) are labelled. Reprinted with permission from *Anal. Chem.* 75 (2003) 2208–2214.^[9] Copyright © 2021, Wiley-VCH.

protein complexes,^[6,81] and comparison of the relative stability of protein mutants.^[82]

An example of how IMS can be combined with temperature-controlled ESI can be seen in the study Woodall et al. (2019).^[79] In this work, TC-ESI-MS was coupled with IMS to elucidate the conformational changes myohemerythrin (Mhr) during thermal denaturation. Eighteen unique conformational intermediates were detected for this protein.^[79] Another interesting finding from this study revealed that apo-myohemerythrin (aMhr) forms a disulfide linkage at temperatures above 80 °C (Figure 5A). Hydroperoxide species with oxidized methionine or cysteine were also detected during this analysis.^[79]

4.2. DNA

Proteins are not the only class of biomolecules that have been examined using TC-ESI-MS. Multiple studies focusing on the thermodynamics of oligonucleotides have also been published. Beginning in the early 2000s, TC-ESI-MS has been used to investigate the structure of oligonucleotides. For example, CSI has been used to spray labile noncovalent oligonucleotide complexes, which could not be analyzed by conventional ESI-MS, due to their low T_m .^[62,66,83] This source was also used to characterize the structure of triple- and quadruple-stranded oligodeoxynucleotides, which could not be detected by other spectroscopic methods.^[84] CSI has also been used to study the binding of a potential anticancer agent, (–)-epigallocatechin gallate, to DNA and RNA.^[85]

This technique has been used to study the secondary structures of DNA, such as double helices, G-quadruplexes (GQ), Z-DNA, cruciform, triplexes, hairpins and the kinetics and stability of 16-mer DNA duplexes.^[86–88] The latter has implications in the production of single-stranded PCR amplicons.^[89] Recent studies have focused on the stability of GQs secondary structures, as they play an important role in DNA replication, transcription, translation and telomere shortening.^[38,90,91] In a recent study by our lab, the stabilization effect of proximal GQ on a duplex DNA was investigated.^[90] Figure 5B shows the melting curves GQ structures (D–G for double helix folded GQ, ss_{D-G} is single strand folded GQ, and ss_{D-G} single strand unfolded GQ) acquired using a temperature ramp from 20 to 80 °C.^[90] This study revealed a two-step unfolding event, with partial unfolding occurring at ~30 °C, and complete unfolding of the GQ at ~60 °C, which highlights this techniques ability to providing insights into mutual domain interactions.^[90] In another recent study, a wire heating TC-ESI-MS source (termed solution thermal melting coupled with ESI) was used to investigate the thermal behavior of RNA assemblies. This worked showed that bis-chloropiperidine is an effective, temperature resistant crosslinker for double stranded RNA.^[92]

4.3. Peptides

The application of TC-ESI-MS to intact peptides is quite recent, and has primarily focused on synthetic collagen peptides,^[8,93] as

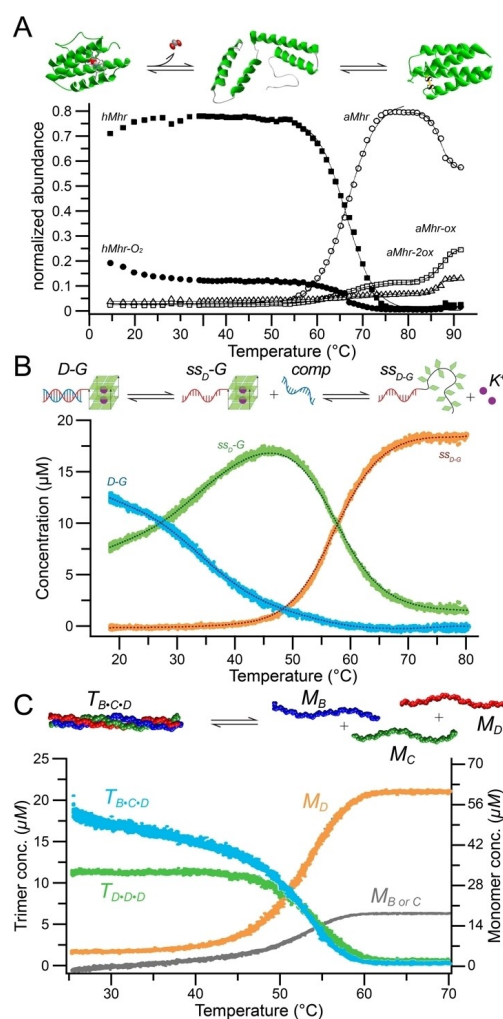


Figure 5. Thermal denaturation profiles of several biological systems. A cartoon of the corresponding chemical equilibrium is depicted on the top of each plot. (A) Structural transformation of peanut worm Mhr in aqueous NH_4Ac solutions from ~15 to 92 °C. As the solution temperature is increased from ~15 to 35 °C, the four-helix bundle motif loses bound oxygen; at ~66 °C, the cofactor dissociates to produce populations of both folded and unfolded apoprotein. At higher temperatures (~85 °C and above), the folded apoprotein dominates, stabilized by a non-native disulfide bond. The plot on the bottom was generated from all charge states of hMhr (■), hMhr- O_2 (●), aMhr (○), aMhr-ox (□), and aMhr-2ox (△). Reprinted with permission from *Anal. Chem.* 2019, 91, 6808.^[95] Copyright © 2021, Wiley-VCH. (B) Thermal denaturation of a DNA two-domain complex consisting of G-quadruplex with an adjacent duplex acquired using TC-nESI-MS. A leading strand (20 μM), complementary strand (20 μM), and KCl (1 mM) was prepared in aqueous buffer of 100 mM TMAA. Melting curves represent fully folded complex (●), the intermediate (●), and the fully unfolded complex (●). Reproduced with permission from *Angew. Chem.*^[90] Copyright © 2021, Wiley-VCH. (C) Thermal unfolding of collagen model peptides forming triple helices from different individual peptide strands ($M_B = \text{Ac}[\text{PKG}]_8\text{-NH}_2$, 2316.39 Da, $M_C = \text{Ac}[\text{DOG}]_8\text{-NH}_2$, 2339.81 Da, $M_D = \text{Ac}[\text{POG}]_8\text{-NH}_2$, 2196.01 Da). The lower panel shows data for the thermal denaturation of two coexisting homotrimeric D-D-D (green) and heterotrimeric B-C-D (orange) helices with $T_{m,MS} = 52$ °C (B-C-D), and $T_{m,MS} = 55$ °C (D-D-D) can be observed; these species all have different m/z and can be easily distinguished by MS. Adapted from *Chem. Sci.* 10 (2019) 9829.^[8] Copyright © 2021, Wiley-VCH.

well as temperature-induced conformational changes and non-enzymatic peptide bond cleavage of bradykinin.^[94] However, there has also been some work done on utilizing high-pressure sources to sequence peptides.

The polydispersity of collagen heterotrimers is a challenge to observe by other biophysical methods.^[8] However, these data can be acquired using TC-ESI-MS. Previous studies by our lab in collaboration with the Wennemers group showed that the high sensitivity of mass spectrometry permits simultaneous detection of multiple species of different mass during thermal denaturation experiments.^[8,93] This is highlighted in Figure 5C, where an increasing spray solution temperature shifts the equilibrium from triple helices (T_{B-C-D} and T_{D-D-D}) to monomeric species (M_D and M_B or M_C), thus allowing for the determination of T_m of each conformation, as well as to determine the heterotrimer subunit composition.^[8]

High-pressure superheated ESI has also been used to investigate peptides by performing thermal degradation of proteins in order to ascertain their peptide sequence.^[11,96,97] This technique has been used to obtain 100% sequence coverage of apo-myoglobin, with all aspartic acid sites cleaved. This source design may provide a useful for ultra-fast high-throughput proteomics experiments.^[96]

5. Conclusion

Over the last few decades, significant progress has been made in the field of mass spectrometry to better understand the behaviour of biomolecular complexes. Recently, the development of temperature-controlled electrospray mass spectrometry (TC-ESI-MS) sources has been driven by new pharmaceutical and biological questions dealing with the interaction and stability of biomolecules, as well as the formation of their complexes. This technique, used in conjunction with conventional assays, has provided detailed insights into the native state, folding mechanisms, and discovery of new intermediates of biomolecules.

Although substantial work has been done using TC-ESI-MS, there are several areas of research, which are likely to be expanded upon. One of these is coupling TC-ESI-MS with ion mobility spectrometry (IMS). This combination has already been used to disentangle multiple folding intermediates, as demonstrated on myohemerythrin.^[79] By applying these techniques to other proteins, peptides and oligonucleotides, a greater understanding of the conformational dynamics of these biomolecules could be achieved. This technique could also be used to investigate enzyme systems. Temperature-induced conformational changes in the enzyme and substrate could be detected using TC-ESI-MS, which could be used to better understand the functional aspects of these enzymes.

There is no research available which directly compares the sources, and there is little cross-over, in terms of biomolecule analyzed, between groups. Due to the absence of said information, it is difficult to directly compare different source designs. Therefore, a comparative analysis between individual TC-ESI-MS designs may be helpful. Such work may help better

determine the advantages/disadvantages of individual systems allowing researchers to choose appropriate instrumentation to investigate biological systems. Eventually, the combination of individual development advantages could lead to commercially available TC-ESI-MS sources. This is of particular importance for sources designed to operate over the boiling point or under the freezing temperature of water. These systems require either complicated cooling systems (low temperature) or a high-pressure ion source chamber (high temperature). Without significant technical expertise, it is difficult to build such devices for laboratories focusing on interactions of biomolecules or protein folding.

Also, better temperature control systems may need to be developed.^[54] To fully address these issues, a new generation of ionization TC-ESI-MS sources may be required. These designs could have the source contained within a sealed chamber (not currently available), allowing for better control of experimental conditions.

Lastly, the increased complexity of TC-ESI-MS data sets creates a demand for software that provides advanced modeling of structures and thermodynamic calculations. The ability to correlate simulation with MS datasets and calculated parameters is essential for the further application of TC-ESI-MS. Although ESI-MS is a sensitive method requiring a low sample amount, a high sample purity is a substantial limitation, which requires demanding and time-consuming sample preparation.

Overall, we hope to have shown in this minireview that TC-ESI-MS is a useful technique for elucidating the structural and thermodynamic characteristics of biomolecules, and it can deliver a wealth of information and complements solution-based standard biophysical methods in an ideal fashion.

Abbreviations

AT	antithrombin
CD	circular dichroism
CMP	collagen model peptide
CSI	cold-spray ionization
DLS	dynamic light scattering
DNA	deoxyribonucleic acid
DSC	differential scanning calorimetry
ESI	electrospray ionization
FP	fluorescence polarization
FRET	Förster resonance energy transfer
GQ	G-quadruplex
HSP	heat-shock protein
IM-MS	ion mobility mass spectrometry
IMS	ion mobility spectrometry
ITC	isothermal titration calorimetry
LAESI	laser ablation electrospray ionization
Mhr	myohemerythrin
MS	mass spectrometry
MST	microscale thermophoresis
nDSF	nano differential scanning fluorimetry
nESI	nano electrospray
NMR	nuclear magnetic resonance

PCR	polymerase chain reaction
PID	proportional-integral-derivative
RNA	ribonucleic acid
SPR	surface plasmon resonance
STHEM	solution thermal melting
TC-ESI	temperature-controlled electrospray
TC-ESI-MS	temperature-controlled electrospray mass spectrometry
TC-nESI	temperature-controlled nanoelectrospray
TC-nESI-MS	temperature-controlled nanoelectrospray mass spectrometry
TD	thermodynamic
TEC	thermoelectric cooler
TMAA	trimethylammonium acetate
UV/Vis	ultraviolet/visible spectroscopy

Acknowledgements

We thank the Swiss National Science Foundation (grant no. 200020_178765) for generous financial support of this work. Open access funding provided by Eidgenössische Technische Hochschule Zurich.

Conflict of Interest

The authors declare no conflict of interest.

Data Availability Statement

Data sharing is not applicable to this article as no new data were created or analyzed in this study.

Keywords: biomolecules · mass spectrometry · structural biology · temperature control · thermodynamics

- [1] N. J. Greenfield, *Nat. Protoc.* **2007**, *1*, 2527–2535.
- [2] N. Berova, L. Di Bari, G. Pescitelli, *Chem. Soc. Rev.* **2007**, *36*, 914–931.
- [3] A. L. Feig, *Methods Enzymol.* **2009**, *468*, 409–422.
- [4] K. A. Vander Meulen, S. Horowitz, R. C. Trievel, S. E. Butcher, in *Methods Enzymol.*, Academic Press Inc., **2016**, pp. 181–213.
- [5] K. Akasaka, A. Naito, H. Nakatani, *J. Biomol. NMR* **1991**, *1*, 65–70.
- [6] T. J. El-Baba, D. W. Woodall, S. A. Raab, D. R. Fuller, A. Laganowsky, D. H. Russell, D. E. Clemmer, *J. Am. Chem. Soc.* **2017**, *139*, 6306–6309.
- [7] G. Wang, R. R. Abzalimov, I. A. Kaltashov, *Anal. Chem.* **2011**, *83*, 2870–2876.
- [8] M. Köhler, A. Marchand, N. B. Hentzen, J. Egli, A. I. Begley, H. Wennemers, R. Zenobi, *Chem. Sci.* **2019**, *10*, 9829–9835.
- [9] J. L. P. Benesch, F. Sobott, C. V. Robinson, *Anal. Chem.* **2003**, *75*, 2208–2214.
- [10] K. Yamaguchi, *J. Mass Spectrom.* **2003**, *38*, 473–490.
- [11] M. M. Rahman, M. K. Mandal, K. Hiraoka, L. C. Chen, *Analyst* **2013**, *138*, 6316–6322.
- [12] A. Marchand, M. F. Czar, E. N. Eggel, J. Kaeslin, R. Zenobi, *Nat. Commun.* **2020**, *11*, 1–12.
- [13] P. S. Santiago, F. Moura, L. M. Moreira, M. M. Domingues, N. C. Santos, M. Tabak, *Biophys. J.* **2008**, *94*, 2228–2240.
- [14] E. R. Simons, E. G. Schneider, E. R. Blout, *J. Biol. Chem.* **1969**, *244*, 4023–4026.
- [15] J. Kypr, I. Kejnovská, D. Renčíuk, M. Vorlíčková, *Nucleic Acids Res.* **2009**, *37*, 1713–1725.
- [16] E. Pinho Melo, M. R. Aires-Barros, S. M. B. Costa, J. M. S. Cabral, *J. Biochem. Biophys. Methods* **1997**, *34*, 45–59.
- [17] N. Poklar, G. Vesnaver, *J. Chem. Educ.* **2000**, *77*, 380–382.
- [18] J. L. Mergny, L. Lacroix, *Curr. Protoc. Nucleic Acid Chem.* **2009**, *17*, 17.1.1–17.1.15.
- [19] C. G. Alexander, R. Wanner, C. M. Johnson, D. Breitsprecher, G. Winter, S. Duhr, P. Baaske, N. Ferguson, *Biochim. Biophys. Acta Proteins Proteomics* **2014**, *1844*, 2241–2250.
- [20] R. Silvers, H. Keller, H. Schwalbe, M. Hengesbach, *ChemBioChem* **2015**, *16*, 1109–1114.
- [21] J. Wen, H. Lord, N. Knutson, M. Wikström, *Anal. Biochem.* **2020**, *593*, 113581.
- [22] M. Jerabek-Willemsen, C. J. Wienken, D. Braun, P. Baaske, S. Duhr, *Assay Drug Dev. Technol.* **2011**, *9*, 342–353.
- [23] C. J. Wienken, P. Baaske, U. Rothbauer, D. Braun, S. Duhr, *Nat. Commun.* **2010**, *1*, 1–7.
- [24] A. Gijsbers, T. Nishigaki, N. Sánchez-Puig, *J. Visualization* **2016**, *2016*, 54640.
- [25] F. Barone, G. Chirico, M. Matzeu, F. Mazzei, F. Pedone, *Eur. Biophys. J.* **1998**, *27*, 137–146.
- [26] K. L. Vedvik, H. C. Eliason, R. L. Hoffman, J. R. Gibson, K. R. Kupcho, R. L. Somberg, K. W. Vogel, *Assay Drug Dev. Technol.* **2004**, *2*, 193–203.
- [27] J. Stetefeld, S. A. McKenna, T. R. Patel, *Biophys. Rev. Lett.* **2016**, *8*, 409–427.
- [28] B. Lorber, F. Fischer, M. Bailly, H. Roy, D. Kern, *Biochem. Mol. Biol. Educ.* **2012**, *40*, 372–382.
- [29] H. H. Nguyen, J. Park, S. Kang, M. Kim, *Sensors (Switzerland)* **2015**, *15*, 10481–10510.
- [30] M. Zekriti, *Plasmonics* **2019**, *14*, 763–768.
- [31] J. E. Redman, *Methods* **2007**, *43*, 302–312.
- [32] F. Cordier, S. Grzesiek, *J. Mol. Biol.* **2002**, *317*, 739–752.
- [33] R. Puglisi, O. Brylski, C. Alfano, S. R. Martin, A. Pastore, P. A. Temussi, *Commun. Chem.* **2020**, *3*, 1–7.
- [34] P. Gill, T. T. Moghadam, B. Ranjbar, *J. Biomol. Tech.* **2010**, *21*, 167–193.
- [35] A. W. P. Vermeer, W. Norde, *Biophys. J.* **2000**, *78*, 394–404.
- [36] G. Wang, P. V. Bondarenko, I. A. Kaltashov, *Analyst* **2018**, *143*, 670–677.
- [37] L. Baranauskienė, J. Matuliene, D. Matulis, *J. Biochem. Biophys. Methods* **2008**, *70*, 1043–1047.
- [38] A. Marchand, F. Rosu, R. Zenobi, V. Gabelica, *J. Am. Chem. Soc.* **2018**, *140*, 12553–12565.
- [39] S. M. Kelly, T. J. Jess, N. C. Price, *Biochim. Biophys. Acta Proteins Proteomics* **2005**, *1751*, 119–139.
- [40] F. Zehender, A. Ziegler, H. J. Schönfeld, J. Seelig, *Biochemistry* **2012**, *51*, 1269–1280.
- [41] L. Konermann, E. Ahadi, A. D. Rodriguez, S. Vahidi, *Anal. Chem.* **2012**, *85*, 2–9.
- [42] R. Beveridge, A. S. Phillips, L. Denbigh, H. M. Saleem, C. E. MacPhee, P. E. Barran, *Proteomics* **2015**, *15*, 2872–2883.
- [43] A. Soleilhac, X. Dagany, P. Dugourd, M. Girod, R. Antoine, *Anal. Chem.* **2015**, *87*, 8210–8217.
- [44] L. De Juan, J. Fernández De La Mora, *J. Colloid Interface Sci.* **1997**, *186*, 280–293.
- [45] J. F. D. La Mora, I. G. Loscertales, *J. Fluid Mech.* **1994**, *260*, 155–184.
- [46] K. Nakagawa, H. Katsuragi, *J. Mass Spectrom. Soc. Jpn.* **1958**, *1958*, 23–25.
- [47] M. Dole, L. L. Mack, R. L. Hines, D. O. Chemistry, R. C. Mobley, L. D. Ferguson, M. B. Alice, *J. Chem. Phys.* **1968**, *49*, 2240–2249.
- [48] C. R. Blakley, J. J. Carmody, M. L. Vestal, *J. Am. Chem. Soc.* **1980**, *102*, 5931–5933.
- [49] J. C. Y. L. Blanc, D. Beuchemin, K. W. M. Siu, R. Guevremont, S. S. Berman, *Org. Mass Spectrom.* **1991**, *26*, 831–839.
- [50] X. Cong, Y. Liu, W. Liu, X. Liang, D. H. Russell, A. Laganowsky, *J. Am. Chem. Soc.* **2016**, *138*, 4346–4349.
- [51] B. Pavlatovská, M. Machálková, P. Brusidová, A. Pruška, K. Štěpka, J. Michálek, T. Nečasová, P. Benes, J. Šmarda, J. Preisler, M. Kozubek, J. Navrátilová, *Front. Oncol.* **2020**, *10*, 2527.
- [52] U. A. Mirza, S. L. Cohen, B. T. Chait, *Anal. Chem.* **1993**, *65*, 1–6.
- [53] T. A. Fligge, M. Przybylski, J. P. Quinn, A. G. Marshall, *Eur. J. Mass Spectrom.* **1998**, *4*, 401–404.
- [54] J. W. McCabe, M. Shirzadeh, T. E. Walker, C.-W. Lin, B. J. Jones, V. H. Wysocki, D. P. Barondeau, D. E. Clemmer, A. Laganowsky, D. H. Russell, *Anal. Chem.* **2021**, *93*, 6924–6931.

- [55] "US Patent for Temperature-controlled electrospray ionization source and methods of use thereof Patent (Patent # 8,766,179 issued July 1, 2014)-Justia Patents Search," can be found under <https://patents.justia.com/patent/8766179>, n.d.
- [56] K. J. Laszlo, J. H. Buckner, E. B. Munger, M. F. Bush, *J. Am. Soc. Mass Spectrom.* **2017**, *28*, 1382–1391.
- [57] K. Jeanne Dit Fouque, F. Fernandez-Lima, *J. Phys. Chem. B* **2020**, *124*, 6257–6265.
- [58] B. Hommersom, T. Porta, R. M. A. Heeren, *Int. J. Mass Spectrom.* **2017**, *419*, 52–55.
- [59] T. J. El-Baba, D. R. Fuller, D. W. Woodall, S. A. Raab, C. R. Conant, J. M. Dilger, Y. Toker, E. R. Williams, D. H. Russell, D. E. Clemmer, *Chem. Commun.* **2018**, *54*, 3270–3273.
- [60] P. Nemes, A. Vertes, *Anal. Chem.* **2007**, *79*, 8098–8106.
- [61] D. W. Woodall, L. W. Henderson, S. A. Raab, K. Honma, D. E. Clemmer, *J. Am. Soc. Mass Spectrom.* **2021**, *32*, 64–72.
- [62] S. Sakamoto, M. Fujita, K. Kim, K. Yamaguchi, *Tetrahedron* **2000**, *56*, 955–964.
- [63] L. C. Chen, M. M. Rahman, K. Hiraoka, *J. Am. Soc. Mass Spectrom.* **2014**, *25*, 1862–1869.
- [64] T. J. El-Baba, D. R. Fuller, D. W. Woodall, S. A. Raab, C. R. Conant, J. M. Dilger, Y. Toker, E. R. Williams, D. H. Russell, D. E. Clemmer, *Chem. Commun.* **2018**, *54*, 3270–3273.
- [65] S. Chen, X. Gong, H. Tan, Y. Liu, L. He, J. Ouyang, *Talanta* **2020**, *211*, 120762.
- [66] S. Sakamoto, K. Yamaguchi, *Tetrahedron Lett.* **2003**, *44*, 3341–3344.
- [67] Y. Sei, S. Shimotakahara, J. Ishii, H. Shindo, H. Seki, K. Yamaguchi, M. Tashiro, *Anal. Sci.* **2005**, *21*, 449–451.
- [68] L. C. Chen, M. K. Mandal, K. Hiraoka, *J. Am. Soc. Mass Spectrom.* **2011**, *22*, 539–544.
- [69] D. J. Miller, S. B. Hawthorne, A. M. Gizir, A. A. Clifford, *J. Chem. Eng. Data* **1998**, *43*, 1043–1047.
- [70] Y. Kostyukevich, G. Ovchinnikov, A. Kononikhin, I. Popov, I. Oseledets, E. Nikolaev, *Int. J. Mass Spectrom.* **2018**, *427*, 100–106.
- [71] J. A. Loo, R. R. O. Loo, H. R. Udseth, C. G. Edmonds, R. D. Smith, *Rapid Commun. Mass Spectrom.* **1991**, *5*, 101–105.
- [72] V. Katta, S. K. Chowdhury, B. T. Chait, *J. Am. Chem. Soc.* **1990**, *112*, 5348–5349.
- [73] S. K. Chowdhury, V. Katta, B. T. Chait, *J. Am. Chem. Soc.* **1990**, *112*, 9012–9013.
- [74] N. Lentze, J. A. Aquilina, M. Lindbauer, C. V. Robinson, F. Narberhaus, *Eur. J. Biochem.* **2004**, *271*, 2494–2503.
- [75] A. J. Painter, N. Jaya, E. Basha, E. Vierling, C. V. Robinson, J. L. P. Benesch, *Chem. Biol.* **2008**, *15*, 246–253.
- [76] R. B. J. Geels, S. Calmat, A. J. R. Heck, S. M. Van Der Vies, R. M. A. Heeren, *Rapid Commun. Mass Spectrom.* **2008**, *22*, 3633–3641.
- [77] G. Li, S. Zheng, Y. Chen, Z. Hou, G. Huang, *Anal. Chem.* **2018**, *90*, 7997–8001.
- [78] X. Cong, Y. Liu, W. Liu, X. Liang, D. H. Russell, A. Laganowsky, *J. Am. Chem. Soc.* **2016**, *138*, 4346–4349.
- [79] D. W. Woodall, T. J. El-Baba, D. R. Fuller, W. Liu, C. J. Brown, A. Laganowsky, D. H. Russell, D. E. Clemmer, *Anal. Chem.* **2019**, *91*, 6808–6814.
- [80] C. J. Brown, D. W. Woodall, T. J. El-Baba, D. E. Clemmer, *J. Am. Soc. Mass Spectrom.* **2019**, *30*, 2438–2445.
- [81] T. J. El-Baba, D. E. Clemmer, *Int. J. Mass Spectrom.* **2019**, *443*, 93–100.
- [82] S. A. Raab, T. J. El-Baba, D. W. Woodall, W. Liu, Y. Liu, Z. Baird, D. A. Hales, A. Laganowsky, D. H. Russell, D. E. Clemmer, *J. Am. Chem. Soc.* **2020**, *142*, 17372–17383.
- [83] K. Metori, Y. Sei, Y. Kimura, T. Ozawa, K. Yamaguchi, M. Miyake, *Chem. Pharm. Bull.* **2005**, *53*, 1029–1033.
- [84] S. Sakamoto, K. Yamaguchi, *Angew. Chem. Int. Ed.* **2003**, *42*, 905–908; *Angew. Chem.* **2003**, *115*, 933–936.
- [85] T. Kuzuhara, Y. Sei, K. Yamaguchi, M. Suganuma, H. Fujiki, *J. Biol. Chem.* **2006**, *281*, 17446–17456.
- [86] J. D. Watson, F. H. C. Crick, *Nature* **1953**, *171*, 737–738.
- [87] M. L. Bochman, K. Paeschke, V. A. Zakian, *Nat. Rev. Genet.* **2012**, *13*, 770–780.
- [88] V. Gabelica, F. Rosu, C. Houssier, E. De Pauw, *Rapid Commun. Mass Spectrom.* **2000**, *14*, 464–467.
- [89] J. B. Mangrum, J. W. Flora, D. C. Muddiman, **2002**.
- [90] A. Pruška, A. Marchand, R. Zenobi, *Angew. Chem. Int. Ed.* **2021**, <https://doi.org/10.1002/anie.202016757>.
- [91] D. Rhodes, H. J. Lipps, *Nucleic Acids Res.* **2015**, *43*, 8627–8637.
- [92] A. Sosic, G. Olivato, C. Carraro, R. Göttlich, D. Fabris, B. Gatto, *Molecules* **2021**, *26*, 1874.
- [93] N. B. Hentzen, V. Islami, M. Köhler, R. Zenobi, H. Wennemers, *J. Am. Chem. Soc.* **2020**, *142*, 2208–2212.
- [94] D. R. Fuller, C. R. Conant, T. J. El-Baba, C. J. Brown, D. W. Woodall, D. H. Russell, D. E. Clemmer, *J. Am. Chem. Soc.* **2018**, *140*, 9357–9360.
- [95] D. W. Woodall, C. J. Brown, S. A. Raab, T. J. El-Baba, A. Laganowsky, D. H. Russell, D. E. Clemmer, *Anal. Chem.* **2020**, *92*, 3440–3446.
- [96] L. C. Chen, S. Ninomiya, K. Hiraoka, *J. Mass Spectrom.* **2016**, *51*, 396–411.
- [97] L. C. Chen, M. Kinoshita, M. Noda, S. Ninomiya, K. Hiraoka, *J. Am. Soc. Mass Spectrom.* **2015**, *26*, 1085–1091.

Manuscript received: July 8, 2021
Accepted manuscript online: October 10, 2021
Version of record online: November 5, 2021